



HAL
open science

Bedload Transport in Laboratory Rivers: the Erosion-Deposition Model

Eric Lajeunesse, Olivier Devauchelle, F. Lachaussée, P. Claudin

► **To cite this version:**

Eric Lajeunesse, Olivier Devauchelle, F. Lachaussée, P. Claudin. Bedload Transport in Laboratory Rivers: the Erosion-Deposition Model. Gravel Bed Rivers 8 - Gravel Bed Rivers and Disasters, Sep 2015, Kyoto and Takayama, Japan. hal-01912426

HAL Id: hal-01912426

<https://hal.science/hal-01912426>

Submitted on 5 Nov 2018

HAL is a multi-disciplinary open access archive for the deposit and dissemination of scientific research documents, whether they are published or not. The documents may come from teaching and research institutions in France or abroad, or from public or private research centers.

L'archive ouverte pluridisciplinaire **HAL**, est destinée au dépôt et à la diffusion de documents scientifiques de niveau recherche, publiés ou non, émanant des établissements d'enseignement et de recherche français ou étrangers, des laboratoires publics ou privés.

Bedload Transport in Laboratory Rivers: the Erosion-Deposition Model

Eric Lajeunesse,^{1, a)} Olivier Devauchelle,¹ F. Lachaussée,¹ and P. Claudin²

¹⁾*Institut de Physique du Globe - Sorbonne Paris Cité,
Equipe de Dynamique des fluides géologiques,
1 rue Jussieu, 75238 Paris cedex 05, France.*

²⁾*Physique et Mécanique des Milieux Hétérogènes, PMMH UMR 7636 ESPCI –
CNRS – Univ. Paris-Diderot – Univ. P.M. Curie, 10 rue Vauquelin, 75005 Paris,
France.*

This chapter is a review of the erosion-deposition model of bedload transport, first proposed by Charru *et al.* (2004). This model, established on the basis of laboratory experiments, proposes a simplified theoretical framework describing the exchange of particles between the sediment bed and the layer of entrained grains. The latter is treated as a uniform reservoir of independent particles moving at velocity V . The exchange of particles between the sediment bed and the bedload layer sets the surface concentration of moving particles, n , and determines the sediment transport rate, $q_s = nV$.

For a steady flow over a wavy topography, the sediment flux adjusts to a change of shear-stress over a characteristic deposition length. This relaxation plays a crucial role in selecting the wavelength of bedforms such as ripples, rhomboid patterns and bars (Andreotti *et al.*, 2012; Charru, 2006; Charru *et al.*, 2013; Charru and Hinch, 2006; Devauchelle *et al.*, 2010b).

The equations describing bedload transport and the development of bedforms are similar in laminar and turbulent flows. This analogy explains why most alluvial morphologies formed in nature also form at a smaller scale when a laminar flow interacts with a sediment bed (Paola *et al.*, 2009).

A preliminary investigation indicates that the erosion-deposition model also accounts for the propagation of a plume of tracers entrained by bedload transport. It suggests that, after a short transient, the plume reaches asymptotically an advection-diffusion regime, in which it advances with a constant velocity while its variance increases linearly with time.

The results discussed in this chapter are based on idealized laboratory experiments (uniform grain size, constant flow and sediment discharges). Rivers, and in particular gravel-bed rivers, often exhibit high grain size heterogeneities and fluctuating flow discharges. Recent progress in extending the erosion-deposition model to the transport of mixed grain sizes should allow us to investigate more realistic configurations (Houssais and Lajeunesse, 2012; Houssais *et al.*, submitted).

Keywords : erosion and deposition in bedload transport, laboratory experiments, alluvial morphology, tracer particles

I. INTRODUCTION

When the shear stress exerted by a river on its bed exceeds a threshold, superficial sediments are entrained by the flow. For moderate values of the shear stress, they move by rolling, sliding and bouncing while gravity maintains them close to the bed surface (Bagnold, 1973). This so-called “bedload transport” deforms the bed, and the resulting interaction between flow and sediment transport generates a beautiful variety of river shapes and coastal morphologies (Church, 2006; Gomez, 1991; Seminara, 2010). Understanding this process requires a sound theory of bedload transport.

Since the pioneering work of Shields (1936), a lot of field, experimental and theoretical work has been devoted to bedload (e.g. Ancey (2010); Ancey *et al.* (2008); Ancey and Heyman (2014); Ashida and Michiue (1973); Bagnold (1956); Bridge and Dominic (1984); Charru *et al.* (2004); Durán *et al.* (2012); Durán *et al.* (2014); Einstein (1950); Engelund and Fredsoe (1976); Fernandez-Luque and Van Beek (1976); Furbish *et al.* (2012a,b,c); Gomez (1991); Gomez and Church (1989); Lajeunesse *et al.* (2010a); Meyer-Peter and Müller (1948); Nino and Garcia (1994); Roseberry *et al.* (2012)). Most studies focus on the prediction of the sediment transport rate at a specific time and location, $q_s(x, t)$. The net exchange of sediment between the bed and the moving layer is then deduced from mass conservation, sometimes referred to as the “Exner equation” in the context of fluvial geomorphology (Seminara, 2010),

$$\frac{\partial h}{\partial t} + \delta v \frac{\partial q_s}{\partial x} = 0 \quad (1)$$

^{a)}lajeunes@ipgp.fr

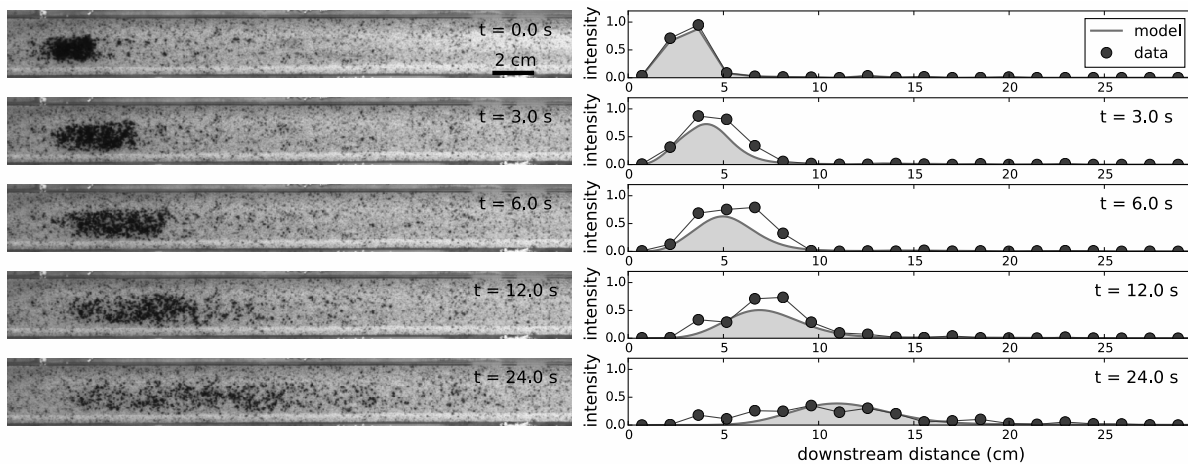


FIG. 1. A plume of dyed sediments in an experimental channel (1 m-long and 3 cm-wide). Left : snapshots of the sediment bed; Right : intensity profiles (dots) averaged along the channel width (levels of grey) used as a proxy for the average tracer concentration. The bed of sediments (plastic grains of size $720 \pm 120 \mu\text{m}$ and density $1520 \pm 50 \text{kg}\cdot\text{m}^{-3}$) is sheared by a mixture of water and glycerol (viscosity $10^{-2} \text{Pa}\cdot\text{s}$ and density $1155 \text{kg}\cdot\text{m}^{-3}$). The flow and sediment discharges, respectively 0.82 l min^{-1} and 0.14 g min^{-1} , are constant during the experiment. The ratio of the concentration of moving particles to the concentration of static particles is $\alpha \sim 8 \cdot 10^{-2}$. The plume of tracers (bed sediments dyed in black) is deposited in the channel once the sediment bed has reached steady-state. Solid line: numerical solution of equations (23) and (24) for $\alpha = 0.08$. The parameters $V = 0.046 \text{m s}^{-1}$ and $t_s = 0.081 \text{s}$ are adjusted to the experimental data.

where we introduce the streamwise coordinate x , the time t , the volume of a sediment particle, δv , and the bed elevation $h(x, t)$. The sediment flux, $q_s(x, t)$, is expressed in number of particles per unit river width and time [$\text{L}^{-1}\text{T}^{-1}$].

To investigate bedload transport, we can use a laboratory channel filled with a bed of plastic sediments (Figure 1). A pump located at the upstream end of the channel sets a steady, uniform and laminar flow entraining the bed sediments. A sediment feeder imposes a constant sediment flux at the channel inlet. After a few hours, the sediment bed reaches a steady-state characterized by a constant slope. We then deposit a plume of dyed sediments at the bed surface and monitor its evolution by means of a camera placed above the channel. We observe that the plume spreads as it is transported downstream (Figure 1). This indicates that the dyed particles move with varied velocities. In particular, some tracer particles initially in motion settle on the bed where they remain trapped. These trapped particles are replaced by sediments freshly entrained from the bed to keep the sediment discharge constant.

These observations suggest a continuous exchange of particles between the sediment bed and the layer of moving grains, referred to as the “bedload layer”. Equation (1) accounts for the evolution of the bed topography. However, it does not explicitly describe the exchange of particles between the bed and the bedload layer which occurs even when the sediment flux is uniform. Yet, this exchange is at the heart of several processes such as the emplacement of alluvial deposits, the determination of the residence time of sediments in a drainage basin and the propagation of sediment tracers in a river bed (Carretier *et al.*, 2007; Gayer *et al.*, 2008; Willenbring and von Blanckenburg, 2010).

Sayre and Hubbell (1965) were the first to experiment sediment tracing in a natural stream. In November 1960, they monitored the propagation of about 18 kg of radioactive sand deposited on the bed of a sandy river in Nebraska (USA). Their data exhibit the same qualitative behaviour as our laboratory experiment : the plume of radioactive sand spreads as it is entrained downstream by the flow (Figure 2).

Since this pioneering work, sediment tracing has become a popular tool to investigate the properties of bedload transport in natural streams (Bradley *et al.*, 2010; Ferguson and Wathen, 1998; Haschenburger and Church, 1998; Reid *et al.*, 1985; Wilcock, 1997). The recent development of radio-frequency identification (RFID) allows the insertion of passive integrated transponders in pebbles (Lamarre *et al.*, 2005; Nichols, 2004). These small electronic tags provide the means to track individual pebble (Figure 3). RFID-tracking is used to study bedload threshold at a fixed location, particle vertical mixing rates, sediment travel lengths, bed and bedforms mobility and particle storage in the sediment bed (Ferguson *et al.*, 2002; Habersack, 2001; Haschenburger and Wilcock, 2003; Hassan *et al.*, 2013; Hodge *et al.*, 2011; Nathan Bradley and Tucker, 2012; Nikora *et al.*, 2002; Phillips and Jerolmack, 2014; Phillips *et al.*, 2013). The interpretation of these observations requires that we understand the exchange of particles between the bed and the bedload layer.

The erosion-deposition model of bedload transport, first proposed by Charru *et al.* (2004), is based on the description

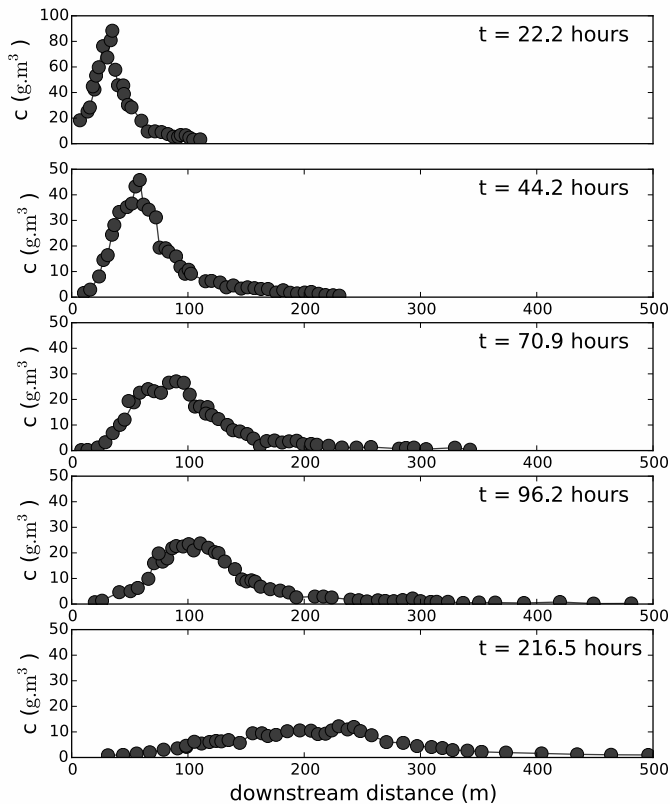


FIG. 2. Evolution of the concentration of radioactive sand injected by Sayre and Hubbell in the North Loup River (Nebraska, USA) in November 1960. After Sayre and Hubbell (1965) and Bradley *et al.* (2010).

of the exchange of particles between the bed and the bedload layer. This heuristic model, inspired by laboratory experiments, describes how this exchange sets the number of moving particles and determines the sediment transport rate (Charru *et al.*, 2004; Lajeunesse *et al.*, 2010a; Seizilles *et al.*, 2014). It is versatile enough to describe the formation of various bedforms, the transport of mixed grain sizes and the propagation of tracers (Charru, 2006; Charru and Hinch, 2006; Devauchelle *et al.*, 2010a,b; Houssais and Lajeunesse, 2012; Lajeunesse *et al.*, 2013).

This chapter is a review of the erosion-deposition model. We begin with a derivation of the model equations based on recent laboratory experiments. We discuss the role of turbulence and the predictions of the model in terms of bedforms development. The chapter ends with a preliminary investigation of the propagation of a plume of tracer sediments.

II. THE EROSION-DEPOSITION MODEL

A. Laboratory observations

Particles entrained by the flow move by rolling, sliding and bouncing until they settle back on the bed. In this paper, we restrict ourselves to the case where the shear stress is close to the entrainment threshold. Image analysis shows that, in this regime, the bedload layer is approximately one grain-diameter thick (Figure 4). This confinement implies that bedload transport is controlled by the characteristics of the flow near the sediment bed. In particular, experiments show that bedload transport is primarily controlled by the ratio of the flow-induced shear stress to the weight of a particle, usually referred to as the Shields parameter (Meyer-Peter and Müller, 1948; Shields, 1936):

$$\theta = \frac{\tau}{(\rho_s - \rho)gd_s} \quad (2)$$

where we introduce the shear stress exerted on the bed τ , the grain size d_s , the sediment density ρ_s , the fluid density ρ and the gravity g . When the Shields parameter exceeds a threshold value, θ_t , the shear stress is strong enough

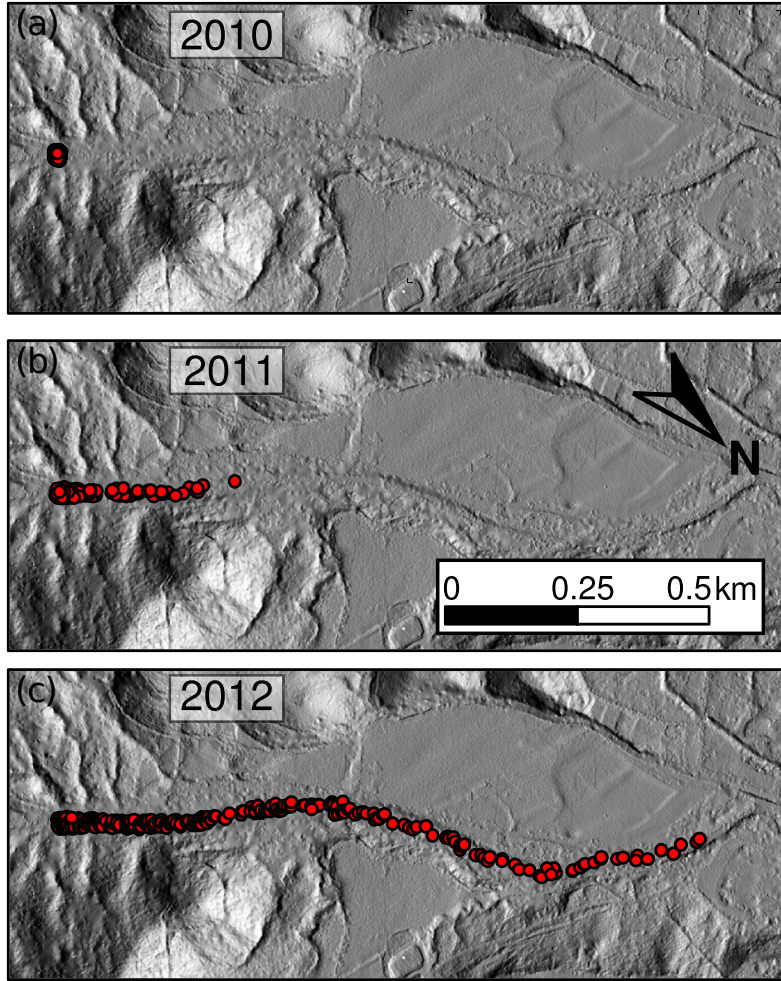


FIG. 3. RFID-tagged pebbles in the Mameyes River (Luquillo Critical Zone Observatory, North East Puerto Rico). Distribution of tracers in (a) May 2010, (b) summer 2011, and (c) summer 2012 (Phillips and Jerolmack, 2014; Phillips *et al.*, 2013). Courtesy of Colin Phillips and Douglas Jerolmack.

to overcome the weight of a particle and to entrain it in the bedload layer. As the Shields stress increases, bedload transport intensifies (Meyer-Peter and Müller, 1948).

The ensemble-averaged sediment transport rate, q_s [$L^{-1}T^{-1}$], can be expressed in terms of the particles velocity distribution,

$$q_s = n \int_0^{\infty} F(v) v dv, \quad (3)$$

where $F(v)$ is the probability distribution function of the particle velocities and $n \ll 1$ is the surface concentration of the bedload layer, i.e. the number of moving particles per unit bed area (Ballio *et al.*, 2014; Furbish *et al.*, 2012b).

Using a camera placed a few centimetres above our experimental channel, we track the grain trajectories and compute their streamwise velocities (Seizilles *et al.*, 2014). The resulting velocity distribution exhibits a peak centred around $v = 0$ with an asymmetric tail on its right side (Figure 5a). Since the camera is placed above the channel, the free surface waves cause a spurious motion which affects even resting particles. We calibrate this noise by plotting the distribution of apparent velocities for static particles (red curve on figure 5a). The result suggests that we may distinguish two populations of particles: (i) particles at rest on the bed corresponding to the central peak on Figure 5a; (ii) particles belonging to the bedload layer corresponding to the distribution tail. Discarding the central peak, an exponential function approximates reasonably the velocity distribution in the bedload layer (figure 5a), in accordance with previous experiments involving either laminar or turbulent flows (figure 5b) (Charru *et al.*, 2004; Furbish *et al.*, 2012b; Lajeunesse *et al.*, 2010a; Seizilles *et al.*, 2014).

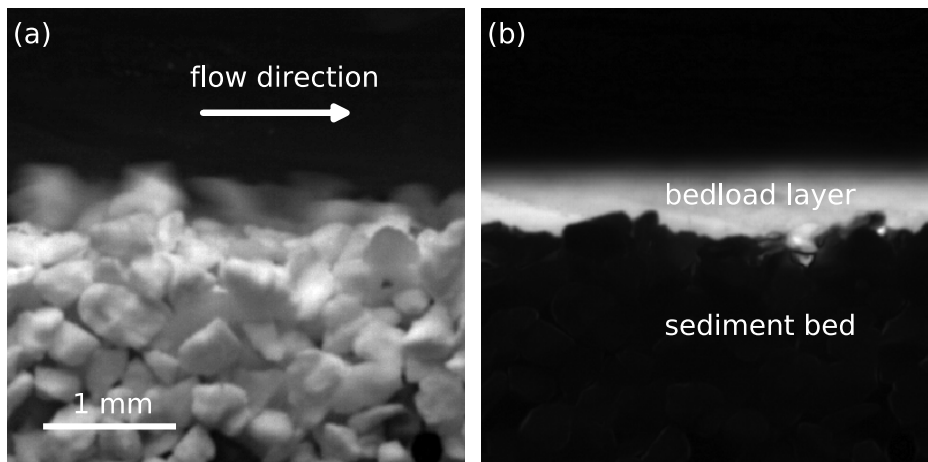


FIG. 4. (a) Side-view of bedload transport in the experimental flume of Figure 1. The sediment bed, made of plastic grains (size $d_s \approx 720 \pm 120 \mu\text{m}$, density $\rho_s = 1520 \pm 50 \text{kg.m}^{-3}$) is sheared by a viscous flow of glycerol (viscosity $\eta = 10^{-2} \text{Pa.s}$, density $\rho = 1155 \text{kg.m}^{-3}$, $\text{Re} \approx 50$). (b) Average amplitude of the difference between two successive pictures. The bedload layer appears in white.

This observation suggests that the streamwise velocity distribution of particles sheared by a flow is the sum of two contributions (Figure 5a),

$$F(v) = \begin{cases} \frac{1}{V} e^{-v/V} & \text{if } v > 0 \\ \delta(v) & \text{otherwise} \end{cases} \quad (4)$$

where $\delta(v)$ is the Dirac function. Equation (4) distinguishes between two reservoirs: (i) the particles at rest represented by a Dirac distribution and (ii) the bedload layer represented by an exponential distribution.

A complete description of sediment transport requires a theoretical formulation of the velocity distribution of particles $F(v)$ and its dependency on the flow conditions (Furbish *et al.*, 2012b). The erosion-deposition model adopts a simplified approach by treating the bedload layer as a uniform reservoir of independent particles moving at velocity V (Charru *et al.*, 2004). Accordingly, the bedload flux equation (3) becomes

$$q_s = nV, \quad (5)$$

To calculate the bedload transport rate, we need to relate the average particle velocity, V , and the surface concentration, n , to the flow conditions.

B. Average particle velocity

The expression of the average particle velocity depends on the flow regime. In a viscous flow, we expect the particles to move at about the velocity of the fluid that entrains them. The average particle velocity should therefore scale with the fluid velocity in the bedload layer, i.e. about one grain diameter above the bed surface,

$$V \propto d_s \frac{\partial u}{\partial z} \quad (6)$$

where we introduce the flow velocity u and the vertical coordinate z . In a viscous flow, the shear rate $\partial u/\partial z$ is proportional to the shear stress, τ , so that

$$V \propto \frac{d_s}{\eta} \tau \propto V_s \theta \quad (7)$$

where η is the fluid viscosity and V_s is the settling velocity of the particle (Charru *et al.*, 2004; Seizilles *et al.*, 2014). Equation (7) accords with experiments (Charru *et al.*, 2004; Lajeunesse *et al.*, 2010a).

In a turbulent flow, one expects the particle velocity to depend on the shear velocity, $u_* = (\tau/\rho)^{1/2} = V_s \theta^{1/2}$. Laboratory experiments and numerical simulations show that

$$V = V_s \left[a(\theta^{1/2} - \theta_t^{1/2}) + b \right]. \quad (8)$$

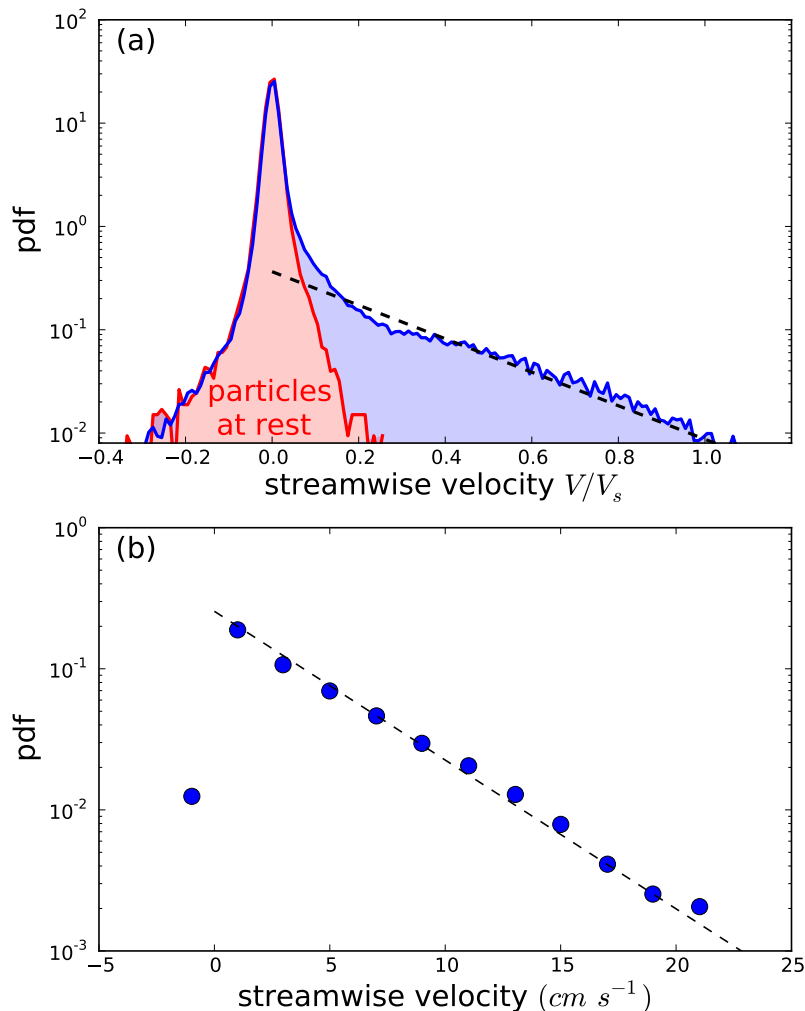


FIG. 5. (a) Streamwise velocity distribution of plastic sediments (density $\rho_s = 1520 \pm 50 \text{ kg.m}^{-3}$, size $d_s = 344 \pm 90 \mu\text{m}$) entrained by a laminar flow (Reynolds number ≈ 500). The velocity distribution (blue curve) is obtained by tracking dyed particles, including those resting on the bed. The spurious noise induced by free surface waves is characterized by the distribution of apparent velocities computed for static particles (red curve). The tail of the velocity distribution is reasonably well fitted by an exponential function (dashed line). After Seizilles *et al.* (2014). (b) Streamwise velocity distribution of sand particles (density $\rho_s = 2500 \text{ kg.m}^{-3}$, size $d_s = 500 \pm 50 \mu\text{m}$) sheared by a turbulent flow (Reynolds number ≈ 30000). Particles are discarded when slower than a small cutoff velocity. The velocity distribution is fitted by an exponential function (dashed line). After Roseberry *et al.* (2012).

where a and b are dimensionless coefficients (Figure 6a) (Durán *et al.*, 2012; Lajeunesse *et al.*, 2010a).

In both laminar and turbulent flows, the average particle velocity, V , scales like the particle settling velocity, V_s , which depends on the flow regime. In a viscous flow, it is the Stoke velocity $V_s = (\rho_s - \rho)gd_s^2 / 18\eta$, whereas it reads $V_s = ((\rho_s - \rho)gd_s / \rho)^{1/2}$ in a turbulent one.

In a laminar flow, the particle velocity tends towards a finite value near threshold (Figure 6b) (Seizilles *et al.*, 2014). This question is still a matter of debate for turbulent flows (Durán *et al.*, 2014; Lajeunesse *et al.*, 2010b).

C. Surface concentration of moving particles

The bedload layer results from a constant exchange of particles with the bed. The associated balance reads (figure 7):

$$\frac{\partial n}{\partial t} + V \frac{\partial n}{\partial x} = \dot{n}_e - \dot{n}_d \quad (9)$$

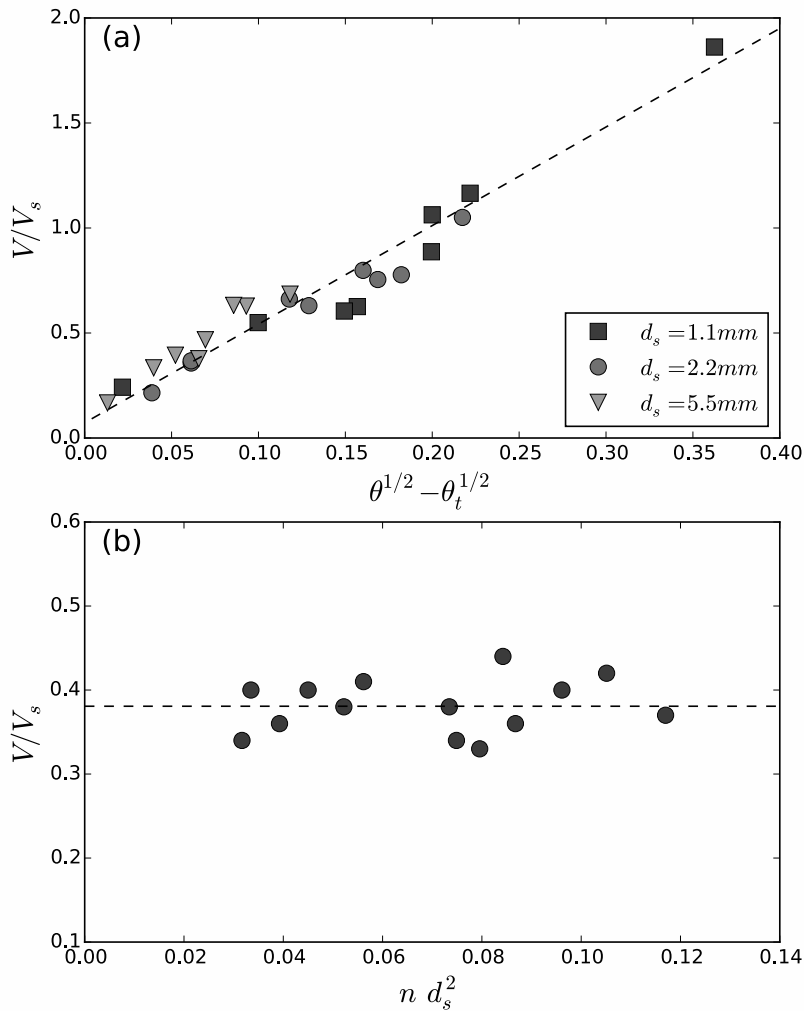


FIG. 6. (a) Average particle velocity, V/V_s , as a function of $(\theta^{1/2} - \theta_t^{1/2})$ for quartz grains in a turbulent flow. A fit of the data by equation (8) (dashed line) leads to $a = 4.4 \pm 0.2$ and $b = 0.11 \pm 0.03$. After Lajeunesse *et al.* (2010a). (b) Average particle velocity, V/V_s , as a function of the concentration of moving sediments, $n d_s^2$, measured near the threshold. Plastic grains (density $\rho_s = 1520 \pm 50\text{kg.m}^{-3}$, size $d_s = 344 \pm 90\mu\text{m}$) are entrained by a laminar flow (Reynolds number ≈ 500). After Seizilles *et al.* (2014).

where we define the erosion rate, \dot{n}_e , as the number of bed particles set in motion per unit time and surface. Similarly, we introduce the deposition rate \dot{n}_d defined as the number of bedload particles settling on the bed per unit time and surface. The mass balance needs to be complemented with expressions for the erosion and deposition rates.

Experimental observations suggest that a particle entrained by the flow bounces on the bed at a rate proportional to d_s/V_s (Charru *et al.*, 2007; Lajeunesse *et al.*, 2010a; Seizilles *et al.*, 2014). Each time the particle hits the bed, it can be trapped with a finite probability. Assuming a uniform probability, the deposition rate scales like the concentration of moving particles times the bouncing frequency:

$$\dot{n}_d \propto n \frac{V_s}{d_s}. \quad (10)$$

Similarly, laboratory experiments suggest that the erosion rate increases with the excess Shields stress, $\theta - \theta_t$ (Charru *et al.*, 2004; Lajeunesse *et al.*, 2010a; Seizilles *et al.*, 2014). At first order, we also expect it to be proportional to the concentration of particles at the bed surface, $\sigma \approx 1/d_s^2$:

$$\dot{n}_e \propto \frac{f(\theta - \theta_t)}{d_s^2} \frac{1}{t_s} \quad (11)$$

where $t_s = d_s/V_s$ and f is a growing function.

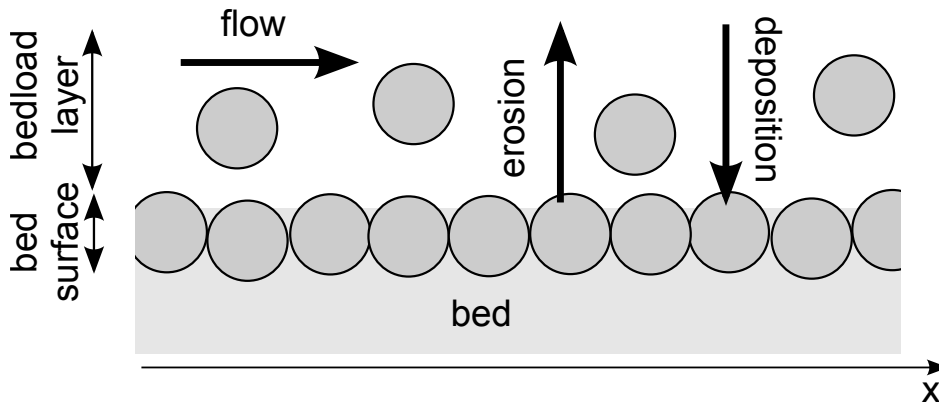


FIG. 7. Granular bed sheared by a laminar flow. Moving grains settle on the bed, while static grains get entrained by the flow.

The form of f can be deduced from steady-state experiments. In this configuration, the mass balance (9) reduces to $f(\theta - \theta_t) \propto n d_s^2$. Measurements of the concentration of bedload particles (see Figure 8) show that f is about linear in both laminar and turbulent flows (Charru *et al.*, 2004; Lajeunesse *et al.*, 2010a; Seizilles *et al.*, 2014). The erosion rate is therefore:

$$\dot{n}_e \propto \frac{1}{d_s^2} \frac{V_s}{d_s} (\theta - \theta_t). \quad (12)$$

D. Bedload transport rate

Equations (5), (6), (9), (10) and (12) describe bedload transport according to the erosion-deposition model. The resolution of these equations for given flow conditions provides the erosion, deposition and bedload transport rates.

In the case of a steady and spatially uniform flow above a flat topography, the erosion and deposition rates balance each other. In this equilibrium regime, the sediment flux reads

$$q_{s,\text{eq}} \propto V d_s (\theta - \theta_t) \quad (13)$$

where the index “eq” denotes equilibrium. The average particle velocity V is given by either (7) or (8) depending on the nature of the flow.

Near the threshold of entrainment, the particle velocity scales as the settling velocity so that the sediment transport rate becomes a linear function of the excess Shields stress,

$$q_s \propto V_s d_s (\theta - \theta_t), \quad (14)$$

in agreement with measurements (Figure 9).

The erosion-deposition model proves reasonable over a broad range of shear stress (Ancey, 2010; Charru *et al.*, 2004; Lajeunesse *et al.*, 2010b). At high shear stress, however, the bedload layer becomes vertically stratified (Durán *et al.*, 2012; Recking *et al.*, 2009). Equation (5) then breaks down, and must be replaced with more detailed diphasic models (e.g. Chiodi *et al.* (2014); Revil-Baudard and Chauchat (2013)).

III. DEPOSITION LENGTH AND BEDFORMS

Rivers exhibit a beautiful variety of bedforms such as ripples, dunes and bars (Charru *et al.*, 2013; Seminara, 2010). These alluvial morphologies result from the feedback between the flow and the bed geometry : (i) the shape of the sediment bed sets the fluid velocity and, therefore, the sediment transport rate; (ii) sediment transport modifies in its turn the shape of the bed.

The mathematical description of this feedback requires an expression for the sediment flux above a wavy bed. When the bed evolves slowly enough, we may consider that the flow is stationary (quasistatic approximation). The shear

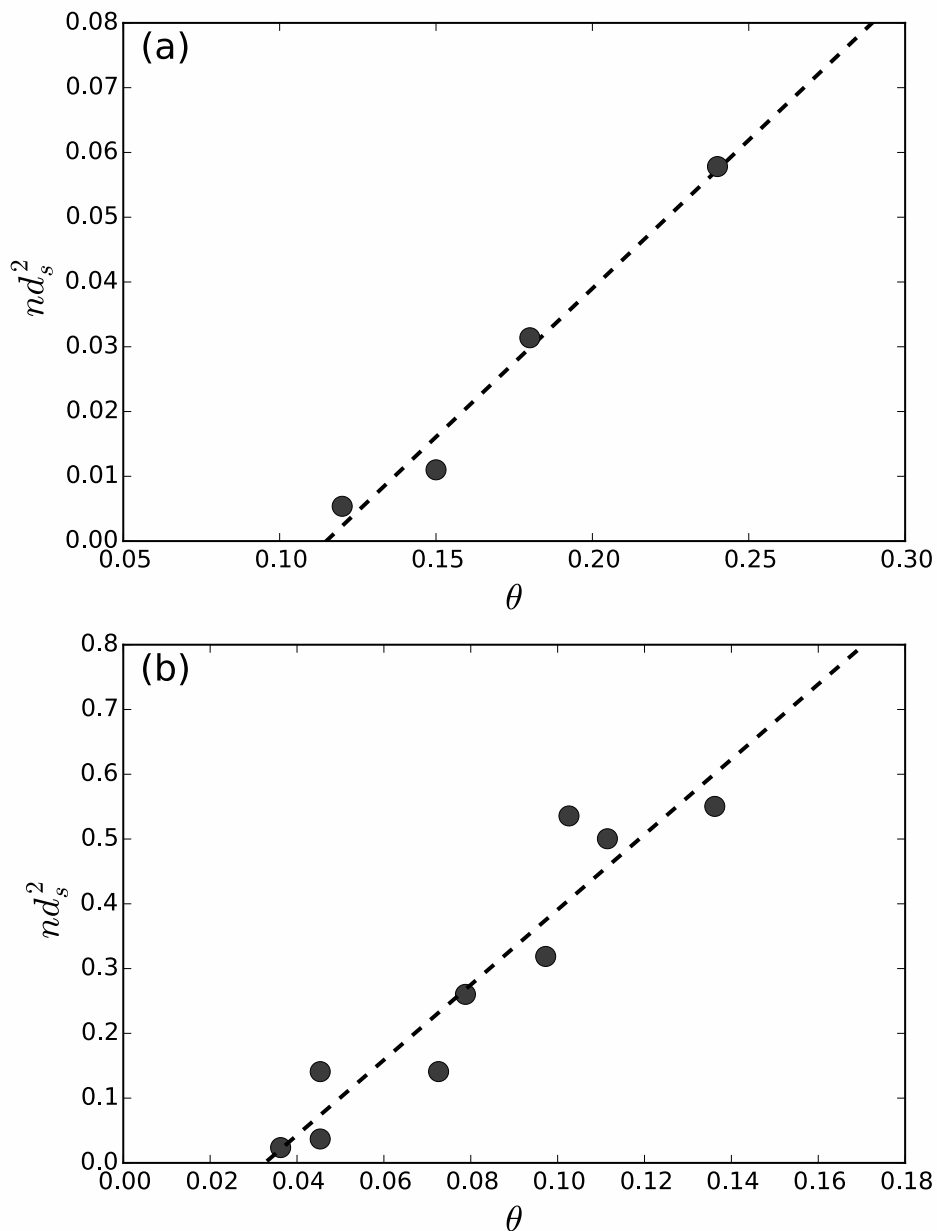


FIG. 8. Surface concentration of moving grains, nd_s^2 , vs Shields number, θ . (a) Spherical acrylic beads (density $\rho_s = 1180 \text{ kg m}^{-3}$, size $d_s = 580 \pm 100 \mu\text{m}$) entrained by a viscous flow of silicon oil (Reynolds number ≈ 40). After Charru *et al.* (2004). (b) Quartz grains (size $d_s = 2.2 \text{ mm}$) entrained by a turbulent flow. After Lajeunesse *et al.* (2010a).

stress then depends on the bed's shape only, and so does the sediment flux. Assuming that particles have negligible inertia, their velocity V adapts instantaneously to the shear stress. Equations (5), (6), (9), (10) and (12) thus reduce to

$$\ell_d \frac{\partial q_s}{\partial x} = q_{s,\text{eq}} - q_s, \quad (15)$$

where $q_{s,\text{eq}}$ is the equilibrium sediment flux predicted from equation (13) and ℓ_d is the average length travelled by a particle before it settles back on the bed ($\ell_d \sim Vt_s \sim Vd_s/V_s$). According to equation (15), the sediment flux adjusts to the local shear-stress over the typical distance ℓ_d . This non-locality of sediment discharge is consistent with other models proposed in the literature (Bell and Sutherland, 1983; Phillips and Sutherland, 1990, 1989). In most of these studies however, non-locality is introduced heuristically. In the erosion-deposition model, it results spontaneously from the exchange of particles between the bed and the bedload layer: entrainment and deposition depend on local

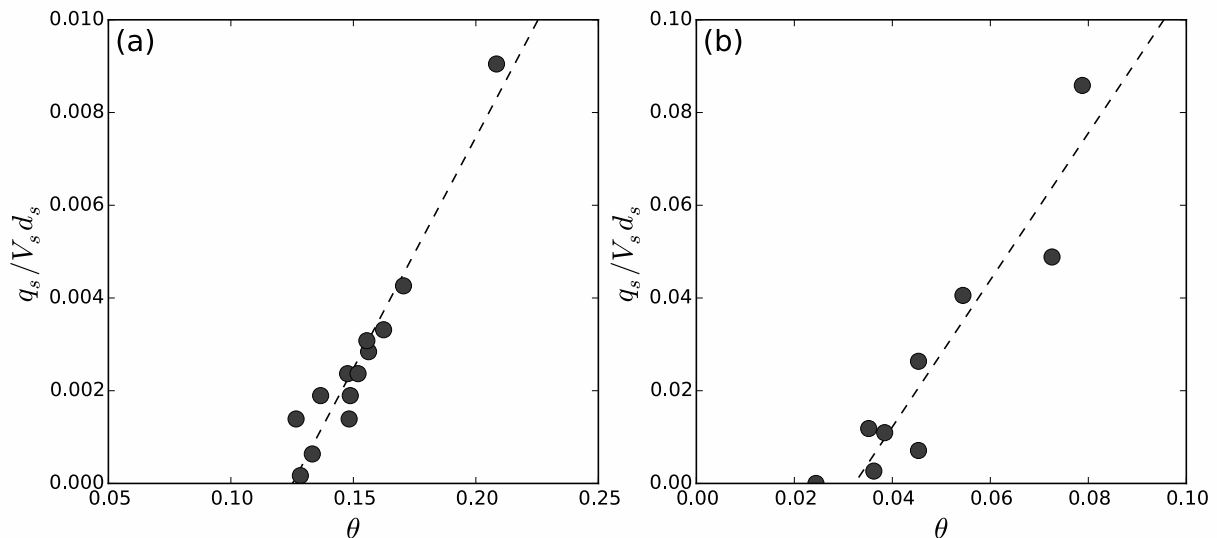


FIG. 9. Sediment transport rate vs Shields number close to the entrainment threshold. (a) plastic sediments (density $\rho_s = 1520 \pm 50 \text{ kg.m}^{-3}$, size $d_s = 344 \pm 90 \mu\text{m}$) entrained by a laminar flow ($\text{Re} \approx 500$). After Seizilles *et al.* (2014). (b) Quartz grains (size $d_s = 2.2 \text{ mm}$) entrained by a turbulent flow. After Lajeunesse *et al.* (2010a).

parameters through equations (10) and (12), and the sediment flux adapts with a delay described by the relaxation equation (15).

The length ℓ_d is analogous to the saturation length introduced in the context of aeolian sand transport where it results from grain inertia and scales like $d_s \rho_s / \rho$, regardless of the wind velocity (Andreotti *et al.*, 2002, 2010; Charru *et al.*, 2013; Claudin and Andreotti, 2006; Hersen, 2005; Narteau *et al.*, 2009; Pähtz *et al.*, 2013; Sauermaun *et al.*, 2001).

Bedload transport generates instabilities: a small perturbation on a flat bed can cause the sediment flux to further increase its size. Charru (2006) successfully describes the early stages of ripple growth in laboratory experiments with a linear stability analysis. The relaxation mechanism embedded in equation (15) introduces a cutoff length which stabilizes the short wavelengths (Fourriere *et al.*, 2010; Kouakou and Lagrée, 2005; Lagrée, 2003; Lagrée *et al.*, 2009). As a result, the size of the most unstable ripples scales with the deposition length ℓ_d , in agreement with experiments (figure 10 a). Similarly, the deposition length seems to control the size of the rhomboid pattern and of alternate bars (figure 10b) (Andreotti *et al.*, 2012; Devauchelle *et al.*, 2010a,b).

Laminar free-surface flows are certainly distinct from turbulent ones in many regards. For instance, the shape of the vertical velocity profile differ between the two, and so does the friction law. However, these quantitative differences do not affect the structure of the associated shallow-water equations (Devauchelle *et al.*, 2007). Similarly, the nature of the flow changes the velocity of bedload particles (equations (7) and (8)), but does not qualitatively alter the mechanism by which the bed exchanges particles with the bedload layer. This analogy explains why many alluvial structures found in nature also form in small laboratory experiments (Coleman and Eling, 2000; Devauchelle *et al.*, 2010a; Guerit *et al.*, 2014; Lajeunesse *et al.*, 2010c; Malverti *et al.*, 2008; Metivier and Meunier, 2003; Paola *et al.*, 2001, 2009; Seizilles *et al.*, 2013).

IV. SPREADING OF A PLUME OF TRACERS

Even in steady state, the bedload layer constantly exchanges particles with the static bed. To illustrate this mechanism, we now consider a plume of tracer particles entrained by bedload transport. We separate the particles into two groups with the same physical properties, hereafter referred to as “marked” and “unmarked”. For the sake of simplicity, we furthermore assume that sediment transport is uniform and steady. In this configuration, equations (5), (6), (9), (10) and (12) predict that the Shields stress (and consequently the mean particle velocity), the erosion and deposition rates and the surface concentration of moving particles are constant. Equation (13) gives the resulting transport rate.

Let us define ϕ as the proportion of marked grains in the moving layer. Similarly, ψ is the proportion of marked grains on the bed surface. The concentration of marked grains, defined as the ratio of the number of marked particles

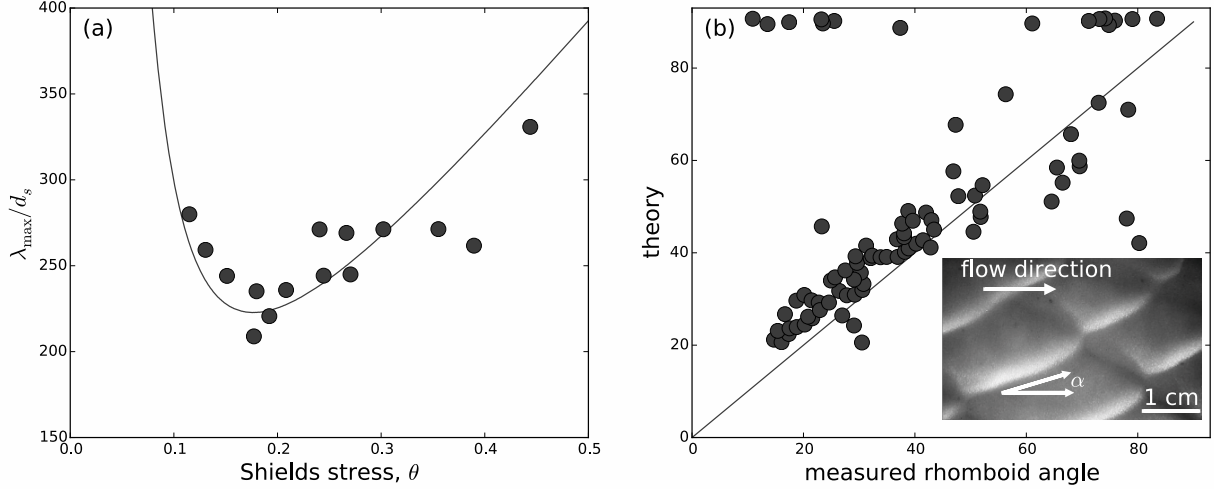


FIG. 10. (a) Ripples wavelength as a function of Shields stress for sand grains in water ($d_s = 200\mu\text{m}$). Dots : experimental measurements by Coleman and Melville (1996). Solid line : prediction of the erosion-deposition model (Charru, 2006). (b) Opening angle α of a rhomboid pattern formed by a viscous flow shearing a bed of glass beads. Dots: comparison between a linear stability analysis and observations. Inset: example of rhomboid pattern. After Devauchelle *et al.* (2010b).

to the surface concentration of particles, is

$$c = \frac{n\phi + \sigma\psi}{n + \sigma} = \frac{\alpha}{\alpha + 1}\phi + \frac{1}{\alpha + 1}\psi \quad (16)$$

where we introduce $\alpha = n/\sigma \sim nd_s^2$, the ratio of the surface concentration of moving particles, n , to the concentration of static particles, σ (this ratio is smaller than one). The total amount of tracers,

$$M = \int_{-\infty}^{\infty} c dx, \quad (17)$$

is conserved. The mass balance for marked grains in the moving layer reads

$$\frac{\partial}{\partial t}(\phi n) + \frac{\partial}{\partial x}(\phi n V) = \dot{n}_e \psi - \dot{n}_d \phi. \quad (18)$$

In steady-state, erosion compensates deposition:

$$\dot{n}_e = \dot{n}_d = \frac{n}{t_s}, \quad (19)$$

where t_s is the characteristic settling time ($t_s \sim d_s/V_s$, see equation 10). Combining equations (18) and (19), we find the evolution equation for the proportion of marked grains in the moving layer:

$$\frac{\partial \phi}{\partial t} + V \frac{\partial \phi}{\partial x} = \frac{1}{t_s}(\psi - \phi). \quad (20)$$

We further assume that the flow can only entrain grains from the bed surface. In other words, the active layer is one-grain-diameter thick. This hypothesis is consistent with a small departure from threshold. Balancing the fluxes of marked grains, we find

$$\sigma \frac{\partial \psi}{\partial t} = \dot{n}_d \phi - \dot{n}_e \psi \quad (21)$$

which, when combined with (19), leads to the evolution equation for the proportion of marked grains on the bed surface:

$$\frac{\partial \psi}{\partial t} = -\frac{\alpha}{t_s}(\psi - \phi). \quad (22)$$

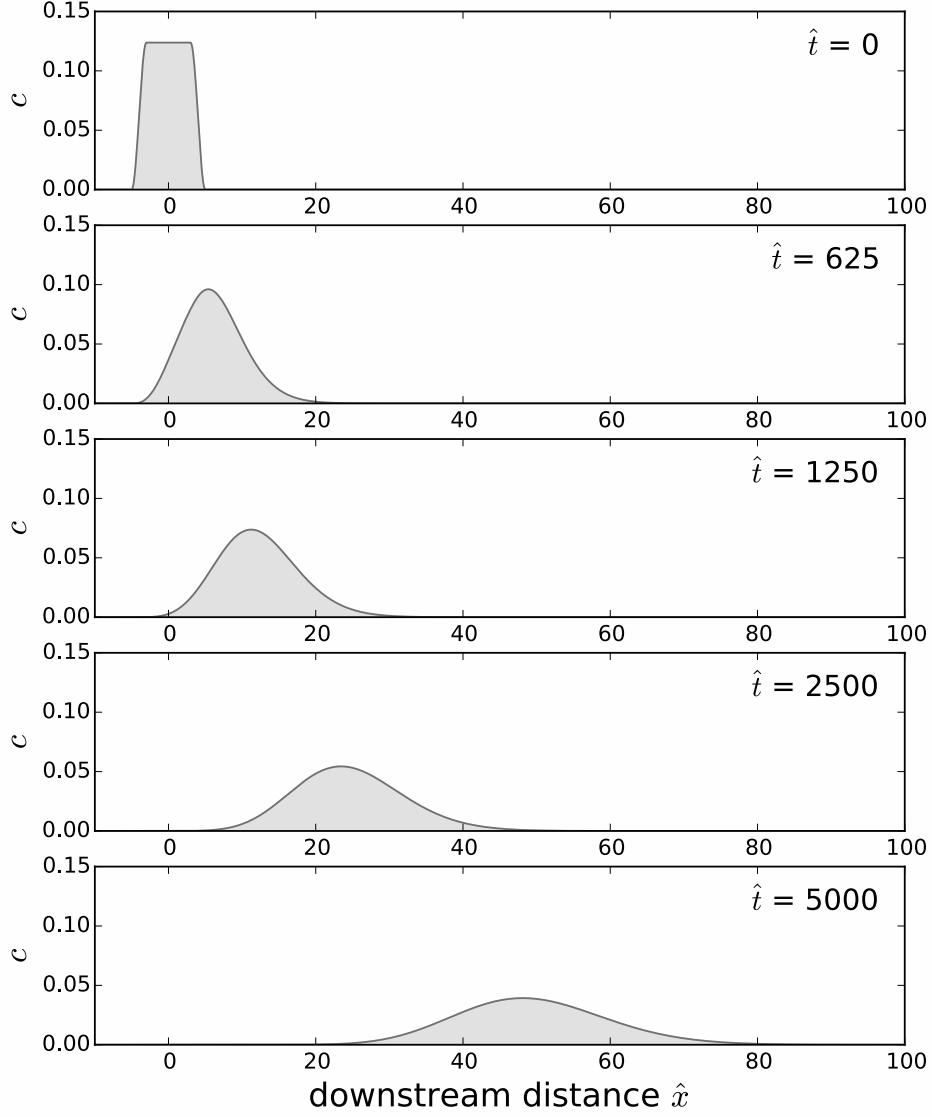


FIG. 11. Numerical computation of the concentration of tracer particles as a function of the dimensionless distance X , for $\alpha = 0.01$. The initial length of the plume is $L = 10$. The concentration is normalized so that the total amount of tracers is 1.

Complemented with initial and boundary conditions, equations (20) and (22) describe the evolution of the plume of marked particles.

In dimensionless form, equations (20) and (22) read

$$\frac{\partial \phi}{\partial \hat{t}} + \frac{\partial \phi}{\partial \hat{x}} = (\psi - \phi) \quad (23)$$

$$\frac{\partial \psi}{\partial \hat{t}} = -\alpha(\psi - \phi). \quad (24)$$

where $\hat{t} = t/t_s$ and $\hat{x} = x/(V t_s)$ are dimensionless variables. A single parameter controls this system of equations: the ratio of surface densities α , which characterizes the average distance between grains in the bedload layer. Since the erosion-deposition model assumes that the behavior of an individual particle is independent from other particles, we can only expect it to be valid when moving particles are sufficiently far away from each other, that is when α is small or, equivalently, when the Shields parameter is near threshold.

We did not measure the ratio of surface densities for the experiment of figure 1. However, its value can be estimated from the sediment flux and the particle settling velocity : $\alpha \sim 8 \cdot 10^{-2}$. We solved equations (23) and (24)

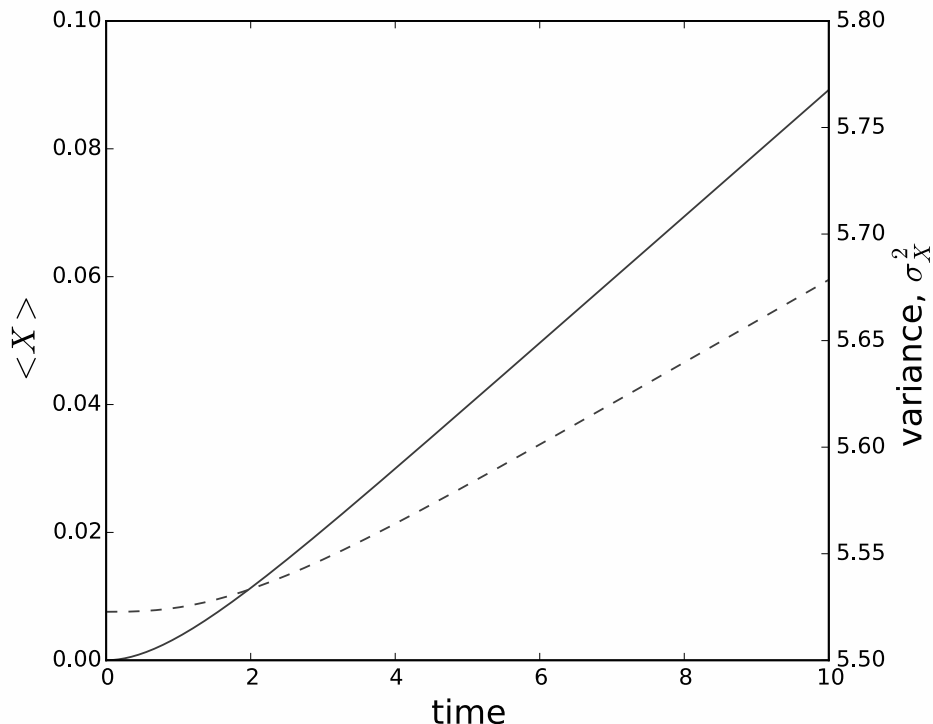


FIG. 12. Mean position $\langle X \rangle$ (solid line, left axis) and variance σ_X^2 (dashed line, right axis) of a plume of tracers as a function of time for the numerical run of Figure 11. After a short transient, the average position and the variance of the plume increase linearly with time.

for $\alpha = 8 \cdot 10^{-2}$ with finite volumes (Lajeunesse *et al.*, 2013). The agreement with experimental data suggests that the erosion-deposition model reasonably represents the plume dynamics.

We now turn our attention to the behaviour of the sediment plume at long times. To do so, we solve numerically equations (23) and (24), starting from an arbitrary configuration, and let it evolve for a long period (Figure 11). As expected, the plume spreads as it is transported downstream by the flow. Initially, its shape is skewed towards the direction of propagation. This skewness later disappears, and the plume resembles a normal distribution at long times.

The average position of the plume, defined as

$$\langle X \rangle = \frac{1}{M} \int_{-\infty}^{\infty} c x dx, \quad (25)$$

increases with time and quickly reaches a constant velocity (figure 12). Similarly, the variance of the plume, defined as

$$\sigma_X^2 = \frac{1}{M} \int_{-\infty}^{\infty} c (x - \langle X \rangle)^2 dx \quad (26)$$

increases linearly with time after a short transient, thus mimicking diffusion. We observe this “effective diffusion” behavior regardless of α . This suggests that, at long times, a plume of tracers advances at constant velocity and diffuses linearly, a behavior reminiscent of the linear advection-diffusion equation. This observation is consistent with the diffusive “intermediate range” regime introduced within the conceptual model of Nikora *et al.* (2002).

In the model presented here, the spread of the plume results only from the continuous exchange of particles between the bedload layer and the immobile bed. In reality, the distribution of particle velocities in bedload transport is continuous (Furbish *et al.*, 2012a,c; Lajeunesse *et al.*, 2010b). Therefore, moving grains in the bedload layer also disperse due to velocity fluctuations. This effect, in addition to the continuous exchange of particles between the bedload layer and the immobile bed, is likely to enhance the dispersion of the plume of tracers.

Although derived in the context of bedload transport, equations (23) and (24) apply to any steady uniform system

in which some passive tracer is exchanged between two layers moving at different velocities. Among such systems are the Taylor dispersion, distillation and chromatography (James *et al.*, 2000; Taylor, 1953).

V. CONCLUSION

Laboratory experiments reveal that, for moderate values of the shear stress, bedload transport involves a continuous exchange of particles between the sediment bed and a thin bedload layer of entrained grains (Charru *et al.*, 2004; Fernandez-Luque and Van Beek, 1976; Lajeunesse *et al.*, 2010b; Nino and Garcia, 1994; Van Rijn, 1984). Taking advantage of this observation and using experimental particle velocity distributions, the erosion-deposition model provides a simple description of bedload transport. The bedload layer is treated as a uniform reservoir of independent particles moving at velocity V (Charru *et al.*, 2004). The exchange of particles between the sediment bed and the bedload layer sets the surface concentration of moving particles, n , and therefore the sediment transport rate, $q_s = nV$.

For a steady flow over a varying topography, the sediment flux adjusts to a change of shear-stress over a characteristic deposition length. This relaxation plays a crucial role in selecting the wavelength of bedforms such as ripples, rhomboids and bars (Charru, 2006; Charru and Hinch, 2006; Devauchelle *et al.*, 2010b). The equations describing bedload transport and the development of bedforms exhibit a strong mathematical analogy in laminar and turbulent flows, thus explaining the “*unreasonable effectiveness of stratigraphic and geomorphic experiments*” (Paola *et al.*, 2009).

A preliminary investigation indicates that the erosion-deposition model also accounts for the propagation of a plume of tracer sediments entrained by bedload transport. It suggests that, after a short transient, the plume reaches asymptotically an advection-diffusion regime, in which it advances with a constant velocity while its variance increases linearly with time. A more quantitative assessment of the model through systematic comparison between theory and experiments is currently under progress.

The results discussed in this chapter are based on idealized laboratory experiments (uniform grain size, constant flow and sediment discharges). The discharge of most rivers, on the other hand, fluctuates significantly throughout the year, and the sediment they transport are often broadly distributed in size. This is specially true for gravel-bed rivers. Recent progress in extending the erosion-deposition model to the transport of mixed grain sizes should allow us to investigate more realistic configurations (Houssais and Lajeunesse, 2012; Houssais *et al.*, submitted).

ACKNOWLEDGEMENT

We are grateful to Colin Phillips and Douglas Jerolmack for the data of Figure 2 and to Francesco Ballio for his insightful review of the manuscript. We also thank F. Mtivier and F. James for fruitful discussions. Part of the experimental work was funded by the SYSTER program of the INSU CNRS.

- Ancey, C. (2010) Stochastic modeling in sediment dynamics: Exner equation for planar bed incipient bed load transport conditions. *J. Geophys. Res.*, **115**, F00A11, doi:10.1029/2009JF001260.
- Ancey, C., Davison, A., Bohm, T., Jodeau, M., and Frey, P. (2008) Entrainment and motion of coarse particles in a shallow water stream down a steep slope. *J. Fluid Mech.*, **595**, 83–114, doi: 10.1017/S0022112007008774.
- Ancey, C. and Heyman, J. (2014) A microstructural approach to bedload transport: mean behavior and fluctuations of particles transport rates. *J. Fluid Mech.*, **744**, 129–168.
- Andreotti, B., Claudin, P., Devauchelle, O., Durán, O., and Fourrière, A. (2012) Bedforms in a turbulent stream: ripples, chevrons and antidunes. *Journal of Fluid Mechanics*, **690**, 94–128.
- Andreotti, B., Claudin, P., and Douady, S. (2002) Selection of dune shapes and velocities part 2: A two-dimensional modelling. *The European Physical Journal B*, **28** (3), 341–352.
- Andreotti, B., Claudin, P., and Pouliquen, O. (2010) Measurements of the aeolian sand transport saturation length. *Geomorphology*, **123** (3), 343–348.
- Ashida, K. and Michiue, M. (1973) Studies on bed-load transport rate in open channel flows, in *IAHR Int. Symp. River Mech.*, Bangkok, 1, pp. 407–417.
- Bagnold, R. (1956) The flow of cohesionless grains in fluids. *Philosophical Transactions of the Royal Society of London. Series A, Mathematical and Physical Sciences*, **249** (964), 235–297.
- Bagnold, R. (1973) The nature of saltation and of bedload transport in water. *Proc. R. Soc. Lond.*, **A 332**, 473–504.
- Ballio, F., Nikora, V., and Coleman, S.E. (2014) On the definition of solid discharge in hydro-environment research and applications. *Journal of Hydraulic Research*, **52** (2), 173–184.
- Bell, R.G. and Sutherland, A.J. (1983) Nonequilibrium bedload transport by steady flows. *Journal of hydraulic engineering*, **109** (3), 351–367.
- Bradley, D.N., Tucker, G.E., and Benson, D.A. (2010) Fractional dispersion in a sand bed river. *Journal of Geophysical Research*, **115**, F00A09.
- Bridge, J. and Dominic, D. (1984) Bed load grain velocity and sediment transport rates. *Water Resources Research*, **20** (4), 476–490.
- Carretier, S., Regard, V., and Soual, C. (2007) In situ cosmogenic nuclides in river bedload. implications for catchment-scale erosion rate and surface exposure dating. *Geochimica et Cosmochimica Acta*, **71** (15), A147–A147.

c	concentration of tracer particles
d_s	sediment size
g	gravity
$F(v)$	probability distribution function of bedload particle velocities
$\ell_d \sim Vt_s \sim Vd_s/V_s$	average flight length travelled by a particle before it settles back on the bed
n	surface concentration of the bedload layer in number of particles per unit bed area
\dot{n}_e	erosion rate in number of particles per unit time and surface
\dot{n}_d	deposition rate in number of particles per unit time and surface
q_s	sediment flux in number of particles per unit river width and time
$q_{s,eq}$	sediment flux in the case of steady and uniform transport
t	time
$t_s \sim d_s/V_s$	characteristic settling time
u_*	shear velocity of the flow
V	average velocity of bedload particles
V_s	sediment settling velocity
x	downstream distance
$\langle X \rangle$	average position of the plume of tracers
$\alpha = n/\sigma$	ratio of the surface concentrations of the bedload layer to the bed surface
η	fluid viscosity
ϕ	proportion of tracers in the moving layer
ψ	proportion of tracers on the bed surface
ρ	fluid density
ρ_s	sediment density
$\sigma \sim 1/d_s^2$	surface concentration of static particles at the bed surface
σ_X^2	variance of the plume of tracers
τ	shear stress exerted by the flow on the bed
θ	Shields number
θ_t	threshold Shields number

TABLE I. List of symbols.

- Charru, F. (2006) Selection of the ripple length on a granular bed sheared by a liquid flow. *Phys. Fluids*, **18**, 121 508–1–121 508–9, doi: 0.1017/S002211200500 786X.
- Charru, F., Andreotti, B., and Claudin, P. (2013) Sand ripples and dunes. *Annual Review of Fluid Mechanics*, **45**, 469–493.
- Charru, F. and Hinch, E. (2006) Ripple formation on a particle bed sheared by a viscous liquid. part 1. steady flow. *J. Fluid Mech.*, **550**, 111–121.
- Charru, F., Larrieu, E., Dupont, J.B., and Zenit, R. (2007) Motion of a particle near a rough wall in a viscous shear flow. *J. Fluid Mech.*, **570**, 431–453.
- Charru, F., Mouilleron, H., and Eiff, O. (2004) Erosion and deposition of particles on a bed sheared by a viscous flow. *Journal of Fluid Mech.*, **519**, 55–80.
- Chiodi, F., Claudin, P., and Andreotti, B. (2014) A two phase flow model of sediment transport: transition from bed-load to suspended-load. *arXiv preprint arXiv:1401.0807*.
- Church, M. (2006) Bed material transport and the morphology of alluvial river channels. *Annu. Rev. Earth Planet. Sci.*, **34**, 325–354.
- Claudin, P. and Andreotti, B. (2006) A scaling law for aeolian dunes on mars, venus, earth, and for subaqueous ripples. *Earth and Planetary Science Letters*, **252** (1), 30–44.
- Coleman, S. and Eling, B. (2000) Sand wavelets in laminar open-channel flows. *Journal of Hydraulic Research*, **38**, 331–338.
- Coleman, S.E. and Melville, B.W. (1996) Initiation of bed forms on a flat sand bed. *Journal of Hydraulic Engineering*, **122** (6), 301–310.
- Devauchelle, O., Josserand, C., Lagrée, P.Y., and Zaleski, S. (2007) Morphodynamic modeling of erodible laminar channels. *Physical Review E*, **76** (5), 056 318.
- Devauchelle, O., Malverti, L., Lajeunesse, E., Josserand, C., Lagrée, P., and Métivier, F. (2010a) Rhomboid beach pattern: A laboratory investigation. *J. Geophys. Res.*, **115**, F02017.
- Devauchelle, O., Malverti, L., Lajeunesse, E., Lagrée, P., Josserand, C., and Thu-Lam, K. (2010b) Stability of bedforms in laminar flows with free surface: from bars to ripples. *Journal of Fluid Mechanics*, **642**, 329–348.
- Durán, O., Andreotti, B., and Claudin, P. (2012) Numerical simulation of turbulent sediment transport, from bed load to saltation. *Phys. Fluids*, **24** (103306).
- Durán, O., Andreotti, B., and Claudin, P. (2014) Turbulent and viscous sediment transport—a numerical study. *Advances in Geosciences*, **37** (37), 73–80.
- Einstein, H. (1950) *The bed-load function for sediment transportation in open channel flows*, US Department of Agriculture. Soil Conservation Service.
- Engelund, F. and Fredsoe, J. (1976) A sediment transport model for straight alluvial channels. *Nordic Hydrol.*, **7** (5), 293–306.
- Ferguson, R. and Wathen, S. (1998) Tracer-pebble movement along a concave river profile: Virtual velocity in relation to grain size and shear stress. *Water Resources Research*, **34** (8), 2031–2038.
- Ferguson, R.I., Bloomer, D.J., Hoey, T.B., and Werritty, A. (2002) Mobility of river tracer pebbles over different timescales. *Water Resources Research*, **38** (5), 3–1.
- Fernandez-Luque, R. and Van Beek, R. (1976) Erosion and transport of bed-load sediment. *Journal of Hydraulic Research*, **14**, 127–144.

- Fourriere, A., Claudin, P., and Andreotti, B. (2010) Bedforms in a turbulent stream: formation of ripples by primary linear instability and of dunes by nonlinear pattern coarsening. *Journal of Fluid Mechanics*, **649**, 287–328.
- Furbish, D., Ball, A., and Schmeeckle, M. (2012a) A probabilistic description of the bed load sediment flux: 4. fickian diffusion at low transport rates. *Journal of Geophysical Research*, **117** (F3), F03034.
- Furbish, D., Haff, P., Roseberry, J., and Schmeeckle, M. (2012b) A probabilistic description of the bed load sediment flux: 1. theory. *Journal of Geophysical Research*, **117** (F3), F03031.
- Furbish, D., Roseberry, J., and Schmeeckle, M. (2012c) A probabilistic description of the bed load sediment flux: 3. the particle velocity distribution and the diffusive flux. *Journal of Geophysical Research*, **117** (F3), F03033.
- Gayer, E., Mukhopadhyay, S., and Meade, B.J. (2008) Spatial variability of erosion rates inferred from the frequency distribution of cosmogenic $^{37}\text{Cl}/^{37}\text{Cl}$ in olivines from hawaiian river sediments. *Earth and Planetary Science Letters*, **266** (3), 303–315.
- Gomez, B. (1991) Bedload transport. *Earth-Science Reviews*, **31** (2), 89–132.
- Gomez, B. and Church, M. (1989) An assessment of bed load sediment transport formulae for gravel bed rivers. *Water Resour. Res.*, **25**, 1161–1186.
- Guerit, L., Métivier, F., Devauchelle, O., Lajeunesse, E., and Barrier, L. (2014) Laboratory alluvial fans in one dimension. *Physical Review E*, **90** (2), 022203.
- Habersack, H. (2001) Radio-tracking gravel particles in a large braided river in new zealand: A field test of the stochastic theory of bed load transport proposed by einstein. *Hydrological Processes*, **15** (3), 377–391.
- Haschenburger, J.K. and Church, M. (1998) Bed material transport estimated from the virtual velocity of sediment. *Earth Surface Processes and Landforms*, **23** (9), 791–808.
- Haschenburger, J.K. and Wilcock, P.R. (2003) Partial transport in a natural gravel bed channel. *Water Resources Research*, **39** (1).
- Hassan, M.A., Voepel, H., Schumer, R., Parker, G., and Fraccarollo, L. (2013) Displacement characteristics of coarse fluvial bed sediment. *Journal of Geophysical Research: Earth Surface*, **118** (1), 155–165.
- Hersen, P. (2005) Flow effects on the morphology and dynamics of aeolian and subaqueous barchan dunes. *J. Geophys. Res.*, **110**, F04S07, doi:10.1029/2004JF000185.
- Hodge, R.A., Hoey, T.B., and Sklar, L.S. (2011) Bed load transport in bedrock rivers: The role of sediment cover in grain entrainment, translation, and deposition. *Journal of Geophysical Research: Earth Surface (2003–2012)*, **116** (F4).
- Houssais, M. and Lajeunesse, E. (2012) Bedload transport of a bimodal sediment bed. *J. Geophys. Res.*, **117**, F04015.
- Houssais, M., Ortiz, C., Durian, D., and Jerolmack, D.J. (submitted) Onset of sediment transport is a continuous transition driven by fluid shear and granular creep. *Nature Physics*.
- James, F., Postel, M., and Sepúlveda, M. (2000) Numerical comparison between relaxation and nonlinear equilibrium models. application to chemical engineering. *Physica D: Nonlinear Phenomena*, **138** (3), 316–333.
- Kouakou, K.K.J. and Lagrée, P.Y. (2005) Stability of an erodible bed in various shear flows. *The European Physical Journal B-Condensed Matter and Complex Systems*, **47** (1), 115–125.
- Lagrée, P.Y. (2003) A triple deck model of ripple formation and evolution. *Physics of Fluids (1994-present)*, **15** (8), 2355–2368.
- Lagrée, P.Y., Devauchelle, O., Nguyen Thu-Lam, K.D., Jossierand, C., Lajeunesse, E., Malverti, L., Métivier, F., and Zaleski, S. (2009) Erosion structures in laminar flumes, in *Powders and grains (2009) Book Series: AIP Conference Proceedings*, vol. 1145 (eds M. Nakagawa and S. Luding), Golden (USA), vol. 1145, pp. 963–966.
- Lajeunesse, E., Devauchelle, O., Houssais, M., and Seizilles, G. (2013) Tracer dispersion in bedload transport. *Adv. Geosci.*, **37**, 1–6.
- Lajeunesse, E., Malverti, L., and Charru, F. (2010a) Bedload transport in turbulent flow at the grain scale: experiments and modeling. *J. Geophys. Res.*, **115**, F04001, doi:10.1029/2009JF001628.
- Lajeunesse, E., Malverti, L., and Charru, F. (2010b) Bedload transport in turbulent flow at the grain scale: experiments and modeling. *J. Geophys. Res. Earth Surface*, **115**, F04001, doi:10.1029/2009JF001628.
- Lajeunesse, E., Malverti, L., Lancien, P., Armstrong, L., Metivier, F., Coleman, S., Smith, C., Davies, T., Cantelli, A., and Parker, G. (2010c) Fluvial and submarine morphodynamics of laminar and near-laminar flows: a synthesis. *Sedimentology*, **57**, 1–26.
- Lamarre, H., MacVicar, B., and Roy, A.G. (2005) Using passive integrated transponder (pit) tags to investigate sediment transport in gravel-bed rivers. *Journal of Sedimentary Research*, **75** (4), 736–741.
- Malverti, L., Lajeunesse, E., and Metivier, F. (2008) Small is beautiful: upscaling microscale experimental results to the size of natural rivers. *J. Geophys. Res.*, **113**, F04004, doi:10.1029/2007JF000974.
- Metivier, F. and Meunier, P. (2003) Input and output mass flux correlations in an experimental braided stream. implications on the dynamics of bed load transport. *Journal of Hydrology*, **271** (1-4), 22–38.
- Meyer-Peter, E. and Müller, R. (1948) Formulas for bed-load transport, in *Proceedings, 2nd Congress, International Association of Hydraulic Research* (ed. S. Stockholm), pp. 39–64.
- Narteau, C., Zhang, D., Rozier, O., and Claudin, P. (2009) Setting the length and time scales of a cellular automaton dune model from the analysis of superimposed bedforms. *J. Geophys. Res. Earth Surface*, **114**, F03006.
- Nathan Bradley, D. and Tucker, G.E. (2012) Measuring gravel transport and dispersion in a mountain river using passive radio tracers. *Earth Surface Processes and Landforms*, **37** (10), 1034–1045.
- Nichols, M. (2004) A radio frequency identification system for monitoring coarse sediment particle displacement. *Applied engineering in agriculture*, **20** (6), 783–787.
- Nikora, V., Habersack, H., Huber, T., and McEwan, I. (2002) On bed particle diffusion in gravel bed flows under weak bed load transport. *Water Resources Research*, **38** (6), 17–1.
- Nino, Y. and Garcia, M. (1994) Gravel saltation. part i: Experiments. *Water Resources Research*, **30** (6), 1907–1914.
- Pächt, T., Kok, J.F., Parteli, E.J., and Herrmann, H.J. (2013) Flux saturation length of sediment transport. *Physical review letters*, **111** (21), 218002.
- Paola, C., Mullin, J., Ellis, C., Mohrig, D., Swenson, J., Parker, G., Hickson, T., Heller, P., Pratson, L., Syvitski, J. et al. (2001) Experimental stratigraphy. *GSA Today*, **11** (7), 4–9.
- Paola, C., Straub, K., Mohrig, D., and Reinhardt, L. (2009) The “unreasonable effectiveness” of stratigraphic and geomorphic experiments. *Earth-Science Reviews*, **97** (1), 1–43.
- Phillips, B. and Sutherland, A. (1990) Temporal lag effect in bed load sediment transport. *Journal of Hydraulic Research*, **28** (1), 5–23.
- Phillips, B.C. and Sutherland, A.J. (1989) Spatial lag effects in bed load sediment transport. *Journal of Hydraulic Research*, **27** (1), 115–133.

- Phillips, C. and Jerolmack, D. (2014) Dynamics and mechanics of bed-load tracer particles. *Earth Surf. Dynam.*, **2**, 513–530.
- Phillips, C.B., Martin, R.L., and Jerolmack, D.J. (2013) Impulse framework for unsteady flows reveals superdiffusive bed load transport. *Geophysical Research Letters*, **40** (7), 1328–1333.
- Recking, A., Frey, P., Paquier, A., and Belleudy, P. (2009) An experimental investigation of mechanisms involved in bed load sheet production and migration. *J. Geophys. Res.*, **114**, F03010, doi:10.1029/2008JF000990.
- Reid, I., Frostick, L.E., and Layman, J.T. (1985) The incidence and nature of bedload transport during flood flows in coarse-grained alluvial channels. *Earth Surface Processes and Landforms*, **10** (1), 33–44.
- Revil-Baudard, T. and Chauchat, J. (2013) A two-phase model for sheet flow regime based on dense granular flow rheology. *Journal of Geophysical Research: Oceans*, **118** (2), 619–634.
- Roseberry, J., Schmeekle, M., and Furbish, D. (2012) A probabilistic description of the bed load sediment flux: 2. particle activity and motions. *Journal of Geophysical Research*, **117** (F3), F03032.
- Saueremann, G., Kroy, K., and Herrmann, H. (2001) Continuum saltation model for sand dunes. *Phys. Rev. E.*, **64** (3; PART 1), 31305–31305.
- Sayre, W. and Hubbell, D. (1965) Transport and dispersion of labeled bed material, north loup river, nebraska, *Tech. Rep. 433-C*, U.S. Geol. Surv. Prof. Pap.
- Seizilles, G., Devauchelle, O., Lajeunesse, E., and Métivier, F. (2013) Width of laminar laboratory rivers. *Phys. Rev. E.*, **87**, 052204.
- Seizilles, G., Lajeunesse, E., Devauchelle, O., and Bak, M. (2014) Cross-stream diffusion in bedload transport. *Phys. of Fluids*, **26** (1), 013302.
- Seminara, G. (2010) Fluvial sedimentary patterns. *Annual Review of Fluid Mechanics*, **42**, 43–66.
- Shields, A.S. (1936) Anwendung der ähnlichkeitsmechanik und der turbulenzforschung auf die geschiebebewegung. *Mitteilung der Preussischen Versuchsanstalt für Wasserbau und Schiffbau*, **26**.
- Taylor, G. (1953) Dispersion of soluble matter in solvent flowing slowly through a tube. *Proceedings of the Royal Society of London. Series A. Mathematical and Physical Sciences*, **219** (1137), 186–203.
- Van Rijn, L. (1984) Sediment transport, part i: bed load transport. *Journal of hydraulic Engineering*, **110** (10), 1431–1456.
- Wilcock, P.R. (1997) Entrainment, displacement and transport of tracer gravels. *Earth Surface Processes and Landforms*, **22** (12), 1125–1138.
- Willenbring, J.K. and von Blanckenburg, F. (2010) Meteoric cosmogenic beryllium-10 adsorbed to river sediment and soil: Applications for earth-surface dynamics. *Earth-Science Reviews*, **98** (1), 105–122.
- Ancey, C. (2010) Stochastic modeling in sediment dynamics: Exner equation for planar bed incipient bed load transport conditions. *J. Geophys. Res.*, **115**, F00A11, doi:10.1029/2009JF001260.
- Ancey, C., Davison, A., Bohm, T., Jodeau, M., and Frey, P. (2008) Entrainment and motion of coarse particles in a shallow water stream down a steep slope. *J. Fluid Mech.*, **595**, 83–114, doi: 10.1017/S0022112007008774.
- Ancey, C. and Heyman, J. (2014) A microstructural approach to bedload transport: mean behavior and fluctuations of particles transport rates. *J. Fluid Mech.*, **744**, 129–168.
- Andreotti, B., Claudin, P., Devauchelle, O., Durán, O., and Fourrière, A. (2012) Bedforms in a turbulent stream: ripples, chevrons and antidunes. *Journal of Fluid Mechanics*, **690**, 94–128.
- Andreotti, B., Claudin, P., and Douady, S. (2002) Selection of dune shapes and velocities part 2: A two-dimensional modelling. *The European Physical Journal B*, **28** (3), 341–352.
- Andreotti, B., Claudin, P., and Pouliquen, O. (2010) Measurements of the aeolian sand transport saturation length. *Geomorphology*, **123** (3), 343–348.
- Ashida, K. and Michiue, M. (1973) Studies on bed-load transport rate in open channel flows, in *IAHR Int. Symp. River Mech., Bangkok, 1*, pp. 407–417.
- Bagnold, R. (1956) The flow of cohesionless grains in fluids. *Philosophical Transactions of the Royal Society of London. Series A, Mathematical and Physical Sciences*, **249** (964), 235–297.
- Bagnold, R. (1973) The nature of saltation and of bedload transport in water. *Proc. R. Soc. Lond.*, **A 332**, 473–504.
- Ballio, F., Nikora, V., and Coleman, S.E. (2014) On the definition of solid discharge in hydro-environment research and applications. *Journal of Hydraulic Research*, **52** (2), 173–184.
- Bell, R.G. and Sutherland, A.J. (1983) Nonequilibrium bedload transport by steady flows. *Journal of hydraulic engineering*, **109** (3), 351–367.
- Bradley, D.N., Tucker, G.E., and Benson, D.A. (2010) Fractional dispersion in a sand bed river. *Journal of Geophysical Research*, **115**, F00A09.
- Bridge, J. and Dominic, D. (1984) Bed load grain velocity and sediment transport rates. *Water Resources Research*, **20** (4), 476–490.
- Carretier, S., Regard, V., and Soual, C. (2007) In situ cosmogenic nuclides in river bedload. implications for catchment-scale erosion rate and surface exposure dating. *Geochimica et Cosmochimica Acta*, **71** (15), A147–A147.
- Charru, F. (2006) Selection of the ripple length on a granular bed sheared by a liquid flow. *Phys. Fluids*, **18**, 121508–1–121508–9, doi: 0.1017/S002211200500786X.
- Charru, F., Andreotti, B., and Claudin, P. (2013) Sand ripples and dunes. *Annual Review of Fluid Mechanics*, **45**, 469–493.
- Charru, F. and Hinch, E. (2006) Ripple formation on a particle bed sheared by a viscous liquid. part 1. steady flow. *J. Fluid Mech.*, **550**, 111–121.
- Charru, F., Larrieu, E., Dupont, J.B., and Zenit, R. (2007) Motion of a particle near a rough wall in a viscous shear flow. *J. Fluid Mech.*, **570**, 431–453.
- Charru, F., Mouilleron, H., and Eiff, O. (2004) Erosion and deposition of particles on a bed sheared by a viscous flow. *Journal of Fluid Mech.*, **519**, 55–80.
- Chiodi, F., Claudin, P., and Andreotti, B. (2014) A two phase flow model of sediment transport: transition from bed-load to suspended-load. *arXiv preprint arXiv:1401.0807*.
- Church, M. (2006) Bed material transport and the morphology of alluvial river channels. *Annu. Rev. Earth Planet. Sci.*, **34**, 325–354.
- Claudin, P. and Andreotti, B. (2006) A scaling law for aeolian dunes on mars, venus, earth, and for subaqueous ripples. *Earth and Planetary Science Letters*, **252** (1), 30–44.
- Coleman, S. and Eling, B. (2000) Sand wavelets in laminar open-channel flows. *Journal of Hydraulic Research*, **38**, 331–338.
- Coleman, S.E. and Melville, B.W. (1996) Initiation of bed forms on a flat sand bed. *Journal of Hydraulic Engineering*, **122** (6), 301–310.

- Devauchelle, O., Josserand, C., Lagrée, P.Y., and Zaleski, S. (2007) Morphodynamic modeling of erodible laminar channels. *Physical Review E*, **76** (5), 056318.
- Devauchelle, O., Malverti, L., Lajeunesse, E., Josserand, C., Lagrée, P., and Métivier, F. (2010a) Rhomboid beach pattern: A laboratory investigation. *J. Geophys. Res.*, **115**, F02017.
- Devauchelle, O., Malverti, L., Lajeunesse, E., Lagrée, P., Josserand, C., and Thu-Lam, K. (2010b) Stability of bedforms in laminar flows with free surface: from bars to ripples. *Journal of Fluid Mechanics*, **642**, 329–348.
- Durán, O., Andreotti, B., and Claudin, P. (2012) Numerical simulation of turbulent sediment transport, from bed load to saltation. *Phys. Fluids*, **24** (103306).
- Durán, O., Andreotti, B., and Claudin, P. (2014) Turbulent and viscous sediment transport—a numerical study. *Advances in Geosciences*, **37** (37), 73–80.
- Einstein, H. (1950) *The bed-load function for sediment transportation in open channel flows*, US Department of Agriculture. Soil Conservation Service.
- Engelund, F. and Fredsoe, J. (1976) A sediment transport model for straight alluvial channels. *Nordic Hydrol.*, **7** (5), 293–306.
- Ferguson, R. and Wathen, S. (1998) Tracer-pebble movement along a concave river profile: Virtual velocity in relation to grain size and shear stress. *Water Resources Research*, **34** (8), 2031–2038.
- Ferguson, R.I., Bloomer, D.J., Hoey, T.B., and Werritty, A. (2002) Mobility of river tracer pebbles over different timescales. *Water Resources Research*, **38** (5), 3–1.
- Fernandez-Luque, R. and Van Beek, R. (1976) Erosion and transport of bed-load sediment. *Journal of Hydraulic Research*, **14**, 127–144.
- Fourriere, A., Claudin, P., and Andreotti, B. (2010) Bedforms in a turbulent stream: formation of ripples by primary linear instability and of dunes by nonlinear pattern coarsening. *Journal of Fluid Mechanics*, **649**, 287–328.
- Furbish, D., Ball, A., and Schmeeckle, M. (2012a) A probabilistic description of the bed load sediment flux: 4. fickian diffusion at low transport rates. *Journal of Geophysical Research*, **117** (F3), F03034.
- Furbish, D., Haff, P., Roseberry, J., and Schmeeckle, M. (2012b) A probabilistic description of the bed load sediment flux: 1. theory. *Journal of Geophysical Research*, **117** (F3), F03031.
- Furbish, D., Roseberry, J., and Schmeeckle, M. (2012c) A probabilistic description of the bed load sediment flux: 3. the particle velocity distribution and the diffusive flux. *Journal of Geophysical Research*, **117** (F3), F03033.
- Gayer, E., Mukhopadhyay, S., and Meade, B.J. (2008) Spatial variability of erosion rates inferred from the frequency distribution of cosmogenic $^{37}\text{Cl}/^{37}\text{Ar}$ in olivines from hawaiian river sediments. *Earth and Planetary Science Letters*, **266** (3), 303–315.
- Gomez, B. (1991) Bedload transport. *Earth-Science Reviews*, **31** (2), 89–132.
- Gomez, B. and Church, M. (1989) An assessment of bed load sediment transport formulae for gravel bed rivers. *Water Resour. Res.*, **25**, 1161–1186.
- Guerit, L., Métivier, F., Devauchelle, O., Lajeunesse, E., and Barrier, L. (2014) Laboratory alluvial fans in one dimension. *Physical Review E*, **90** (2), 022203.
- Habersack, H. (2001) Radio-tracking gravel particles in a large braided river in new zealand: A field test of the stochastic theory of bed load transport proposed by einstein. *Hydrological Processes*, **15** (3), 377–391.
- Haschenburger, J.K. and Church, M. (1998) Bed material transport estimated from the virtual velocity of sediment. *Earth Surface Processes and Landforms*, **23** (9), 791–808.
- Haschenburger, J.K. and Wilcock, P.R. (2003) Partial transport in a natural gravel bed channel. *Water Resources Research*, **39** (1).
- Hassan, M.A., Voepel, H., Schumer, R., Parker, G., and Fraccarollo, L. (2013) Displacement characteristics of coarse fluvial bed sediment. *Journal of Geophysical Research: Earth Surface*, **118** (1), 155–165.
- Hersen, P. (2005) Flow effects on the morphology and dynamics of aeolian and subaqueous barchan dunes. *J. Geophys. Res.*, **110**, F04S07, doi:10.1029/2004JF000185.
- Hodge, R.A., Hoey, T.B., and Sklar, L.S. (2011) Bed load transport in bedrock rivers: The role of sediment cover in grain entrainment, translation, and deposition. *Journal of Geophysical Research: Earth Surface (2003–2012)*, **116** (F4).
- Houssais, M. and Lajeunesse, E. (2012) Bedload transport of a bimodal sediment bed. *J. Geophys. Res.*, **117**, F04015.
- Houssais, M., Ortiz, C., Durian, D., and Jerolmack, D.J. (submitted) Onset of sediment transport is a continuous transition driven by fluid shear and granular creep. *Nature Physics*.
- James, F., Postel, M., and Sepúlveda, M. (2000) Numerical comparison between relaxation and nonlinear equilibrium models. application to chemical engineering. *Physica D: Nonlinear Phenomena*, **138** (3), 316–333.
- Kouakou, K.K.J. and Lagrée, P.Y. (2005) Stability of an erodible bed in various shear flows. *The European Physical Journal B-Condensed Matter and Complex Systems*, **47** (1), 115–125.
- Lagrée, P.Y. (2003) A triple deck model of ripple formation and evolution. *Physics of Fluids (1994–present)*, **15** (8), 2355–2368.
- Lagrée, P.Y., Devauchelle, O., Nguyen Thu-Lam, K.D., Josserand, C., Lajeunesse, E., Malverti, L., Métivier, F., and Zaleski, S. (2009) Erosion structures in laminar flumes, in *Powders and grains (2009) Book Series: AIP Conference Proceedings*, vol. 1145 (eds M. Nakagawa and S. Luding), Golden (USA), vol. 1145, pp. 963–966.
- Lajeunesse, E., Devauchelle, O., Houssais, M., and Seizilles, G. (2013) Tracer dispersion in bedload transport. *Adv. Geosci.*, **37**, 1–6.
- Lajeunesse, E., Malverti, L., and Charru, F. (2010a) Bedload transport in turbulent flow at the grain scale: experiments and modeling. *J. Geophys. Res.*, **115**, F04001, doi:10.1029/2009JF001628.
- Lajeunesse, E., Malverti, L., and Charru, F. (2010b) Bedload transport in turbulent flow at the grain scale: experiments and modeling. *J. Geophys. Res. Earth Surface*, **115**, F04001, doi:10.1029/2009JF001628.
- Lajeunesse, E., Malverti, L., Lancien, P., Armstrong, L., Metivier, F., Coleman, S., Smith, C., Davies, T., Cantelli, A., and Parker, G. (2010c) Fluvial and submarine morphodynamics of laminar and near-laminar flows: a synthesis. *Sedimentology*, **57**, 1–26.
- Lamarre, H., MacVicar, B., and Roy, A.G. (2005) Using passive integrated transponder (pit) tags to investigate sediment transport in gravel-bed rivers. *Journal of Sedimentary Research*, **75** (4), 736–741.
- Malverti, L., Lajeunesse, E., and Metivier, F. (2008) Small is beautiful: upscaling microscale experimental results to the size of natural rivers. *J. Geophys. Res.*, **113**, F04004, doi:10.1029/2007JF000974.
- Metivier, F. and Meunier, P. (2003) Input and output mass flux correlations in an experimental braided stream. implications on the dynamics of bed load transport. *Journal of Hydrology*, **271** (1-4), 22–38.
- Meyer-Peter, E. and Müller, R. (1948) Formulas for bed-load transport, in *Proceedings, 2nd Congress, International Association of Hydraulic Research* (ed. S. Stockholm), pp. 39–64.

- Narteau, C., Zhang, D., Rozier, O., and Claudin, P. (2009) Setting the length and time scales of a cellular automaton dune model from the analysis of superimposed bedforms. *J. Geophys. Res. Earth Surface*, **114**, F03006.
- Nathan Bradley, D. and Tucker, G.E. (2012) Measuring gravel transport and dispersion in a mountain river using passive radio tracers. *Earth Surface Processes and Landforms*, **37** (10), 1034–1045.
- Nichols, M. (2004) A radio frequency identification system for monitoring coarse sediment particle displacement. *Applied engineering in agriculture*, **20** (6), 783–787.
- Nikora, V., Habersack, H., Huber, T., and McEwan, I. (2002) On bed particle diffusion in gravel bed flows under weak bed load transport. *Water Resources Research*, **38** (6), 17–1.
- Nino, Y. and Garcia, M. (1994) Gravel saltation. part i: Experiments. *Water Resources Research*, **30** (6), 1907–1914.
- Pähtz, T., Kok, J.F., Parteli, E.J., and Herrmann, H.J. (2013) Flux saturation length of sediment transport. *Physical review letters*, **111** (21), 218002.
- Paola, C., Mullin, J., Ellis, C., Mohrig, D., Swenson, J., Parker, G., Hickson, T., Heller, P., Pratson, L., Syvitski, J. *et al.* (2001) Experimental stratigraphy. *GSA Today*, **11** (7), 4–9.
- Paola, C., Straub, K., Mohrig, D., and Reinhardt, L. (2009) The “unreasonable effectiveness” of stratigraphic and geomorphic experiments. *Earth-Science Reviews*, **97** (1), 1–43.
- Phillips, B. and Sutherland, A. (1990) Temporal lag effect in bed load sediment transport. *Journal of Hydraulic Research*, **28** (1), 5–23.
- Phillips, B.C. and Sutherland, A.J. (1989) Spatial lag effects in bed load sediment transport. *Journal of Hydraulic Research*, **27** (1), 115–133.
- Phillips, C. and Jerolmack, D. (2014) Dynamics and mechanics of bed-load tracer particles. *Earth Surf. Dynam.*, **2**, 513–530.
- Phillips, C.B., Martin, R.L., and Jerolmack, D.J. (2013) Impulse framework for unsteady flows reveals superdiffusive bed load transport. *Geophysical Research Letters*, **40** (7), 1328–1333.
- Recking, A., Frey, P., Paquier, A., and Belleudy, P. (2009) An experimental investigation of mechanisms involved in bed load sheet production and migration. *J. Geophys. Res.*, **114**, F03010, doi:10.1029/2008JF000990.
- Reid, I., Frostick, L.E., and Layman, J.T. (1985) The incidence and nature of bedload transport during flood flows in coarse-grained alluvial channels. *Earth Surface Processes and Landforms*, **10** (1), 33–44.
- Revil-Baudard, T. and Chauchat, J. (2013) A two-phase model for sheet flow regime based on dense granular flow rheology. *Journal of Geophysical Research: Oceans*, **118** (2), 619–634.
- Roseberry, J., Schmeckle, M., and Furbish, D. (2012) A probabilistic description of the bed load sediment flux: 2. particle activity and motions. *Journal of Geophysical Research*, **117** (F3), F03032.
- Saueremann, G., Kroy, K., and Herrmann, H. (2001) Continuum saltation model for sand dunes. *Phys. Rev. E.*, **64** (3; PART 1), 31305–31305.
- Sayre, W. and Hubbell, D. (1965) Transport and dispersion of labeled bed material, north loup river, nebraska, *Tech. Rep. 433-C*, U.S. Geol. Surv. Prof. Pap.
- Seizilles, G., Devauchelle, O., Lajeunesse, E., and Métivier, F. (2013) Width of laminar laboratory rivers. *Phys. Rev. E.*, **87**, 052204.
- Seizilles, G., Lajeunesse, E., Devauchelle, O., and Bak, M. (2014) Cross-stream diffusion in bedload transport. *Phys. of Fluids*, **26** (1), 013302.
- Seminara, G. (2010) Fluvial sedimentary patterns. *Annual Review of Fluid Mechanics*, **42**, 43–66.
- Shields, A.S. (1936) Anwendung der aehnlichkeitsmechanik und der turbulenzforschung auf die geschiebbewegung. *Mitteilung der Preussischen Versuchsanstalt fur Wasserbau und Schiffbau*, **26**.
- Taylor, G. (1953) Dispersion of soluble matter in solvent flowing slowly through a tube. *Proceedings of the Royal Society of London. Series A. Mathematical and Physical Sciences*, **219** (1137), 186–203.
- Van Rijn, L. (1984) Sediment transport, part i: bed load transport. *Journal of hydraulic Engineering*, **110** (10), 1431–1456.
- Wilcock, P.R. (1997) Entrainment, displacement and transport of tracer gravels. *Earth Surface Processes and Landforms*, **22** (12), 1125–1138.
- Willenbring, J.K. and von Blanckenburg, F. (2010) Meteoric cosmogenic beryllium-10 adsorbed to river sediment and soil: Applications for earth-surface dynamics. *Earth-Science Reviews*, **98** (1), 105–122.